npj | 2D materials and applications

www.nature.com/npj2dmaterials

ARTICLE OPEN

Transfer-free rapid growth of 2-inch wafer-scale patterned graphene as transparent conductive electrodes and heat spreaders for GaN LEDs

Fangzhu Xiong[1], Jie Sun[2,3]✉, Penghao Tang[1], Weiling Guo[1], Yibo Dong[1], Zaifa Du[1], Shiwei Feng[1] and Xuan Li[1]

A technique for the transfer-free growth of 2-inch wafer-scale patterned graphene directly on GaN LED epilayers is introduced. High-quality graphene as transparent electrodes and heat spreaders is synthesized directly on GaN by PECVD at only 600 °C deposition temperature and within 3 min growth time. Co acts as both the catalyst for graphene growth and the dry etching mask for GaN mesas, which greatly improves the efficiency of the semiconductor device process. Elegantly, the graphene growth is in accordance with the shape of Co, which offers a lithography-free patterning technique of the graphene. Afterward, using our penetration etching method through the PMMA and graphene layers, the Co is peacefully removed, and in-situ Ohmic contact is achieved between the graphene and p-GaN where the contact resistivity is only 0.421 Ω cm^2. The graphene sheet resistance is as low as 631.2 Ω sq^{-1}. The device is also superior to the counterpart graphene-free LED in terms of heat spreading behavior, as evidenced by the lower junction temperature and thermal resistance. Most importantly, the developed technique produces graphene with excellent performance and is intrinsically more scalable, controllable, and semiconductor industry compatible than traditionally transferred graphene.

npj 2D Materials and Applications (2023)7:72 ; https://doi.org/10.1038/s41699-023-00434-9

INTRODUCTION

Graphene is a two-dimensional (2D) material with high carrier mobility, high transmittance, and great thermal conductivity[1–4], has become the most promising candidate to replace indium tin oxide (ITO) as a transparent electrode on gallium nitride (GaN) light emitting diode (LED) applications[5]. In order to avoid complex transfer processes of graphene and efficiently apply to large-scale industrial production, currently, there are two main directions to the growth chemical vapor deposition(CVD) graphene films on GaN directly, One is to synthesize non-catalytic graphene directly on the surface of GaN at high temperatures[6–9]. In fact, our group has carried out the pioneer work of directly growing graphene on GaN wafers in 2012[7]. However, due to the lack of metal catalysts and the lattice mismatch between GaN and graphene, it is really hard to obtain high-quality graphene films directly on GaN. Also, buckling and decomposition will occur in GaN substrate due to the high temperature CVD[6], which caused the irreversible damage to the performance of the LED. Another method is to grow graphene by using metal catalysis[10–12], but the graphene here is grown on the surface of the metal which is deposited on GaN, instead of growing on GaN directly. The metal here can not be removed easily, because graphene will float on the surface of the etching solution after the metal is removed, turning this process back to a manual transfer instead of a transfer-free process. Furthermore, it is well known that metal is highly opaque, so the high transparency will be hard to obtain in metal/graphene composite electrodes, if one dose not remove the metal. Therefore, currently, all the reported directly grown graphene on GaN has serious shortcomings free method of forming graphene on GaN with decent quality[13,14]. In addition, since self-heating is a severe problem for GaN substrate, whose thermal conductivity ranges from ~ 125 to 225 W m^{-1} K^{-1}[15,16], graphene can play a fully advantage on heat spreading which can ideally reach 5300 W m^{-1}K^{-1} at RT (room temperature)[4], which, unfortunately, is rarely reported in previous graphene coated GaN LED research.

Based on theses backgrounds, we invent a method to remove the metal catalyst and make the graphene falls on the GaN automatically without any manual transfer process. In our process, a PMMA (poly(methyl methacrylate)) layer is spin-coated onto the graphene that is deposited on the metal atop the GaN, which can be used as a support layer for graphene, so that the graphene would naturally fall on the GaN after the metal is removed. The etching solution can pass through the graphene and PMMA to etch the metal. Besides, the metal here acts as both a catalyst for graphene growth and a mask for GaN etching. The graphene thus grows rapidly into patterns without lithography, and is avoided with contacting the photoresist, which improves the process efficiency. This methods is highly repeatable. Large-scale graphene arrays as transparent conductive electrodes with efficiently heat spreading effect can be evenly obtained on GaN directly at low temperatures, and with short growth time in the plasma enhanced CVD. Furthermore, this method is also expected to be applied to other 2D materials and devices, and may led to a high impact in pushing the 2D material research towards real scalable electronic applications.

RESULTS AND DISCUSSION

Graphene characterization and analysis

After obtaining the PECVD graphene films directly on p-GaN by the penetration etching in Fig. 1, the film properties are

[1]Key Laboratory of Optoelectronics Technology, College of Microelectronics, Beijing University of Technology, Beijing, China. [2]Fujian Science & Technology Innovation Laboratory for Optoelectronic Information of China, and National and Local United Engineering Laboratory of Flat Panel Display Technology, College of Physics and Information Engineering, Fuzhou University, Fuzhou, China. [3]Quantum Device Physics Laboratory, Department of Microscience and Nanotechnology, Chalmers University of Technology, Göteborg, Sweden. ✉email: jie.sun@fzu.edu.cn

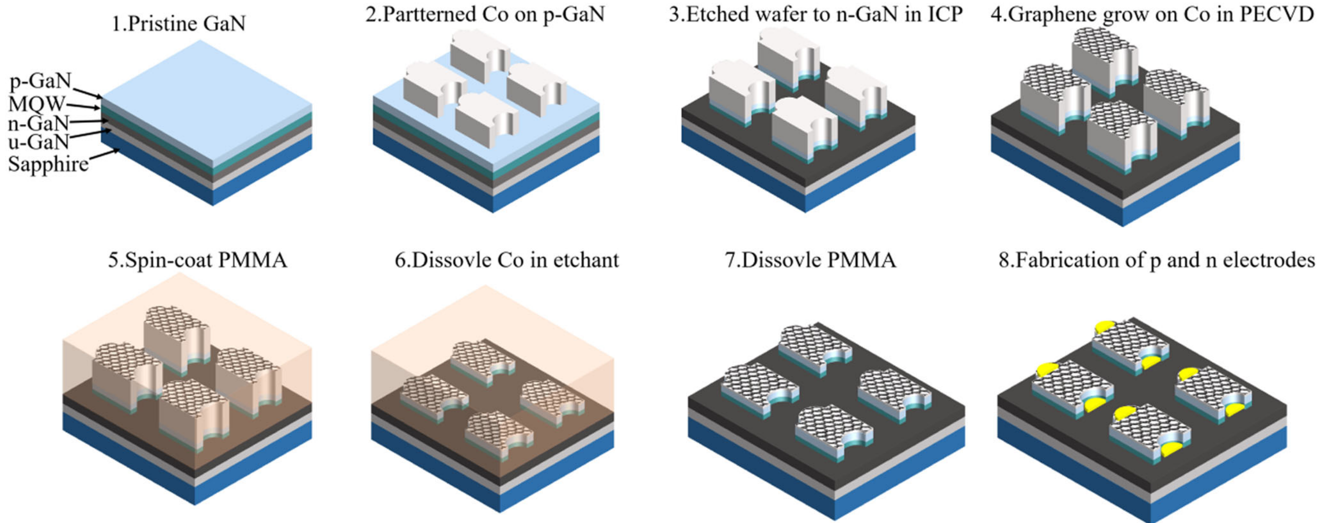

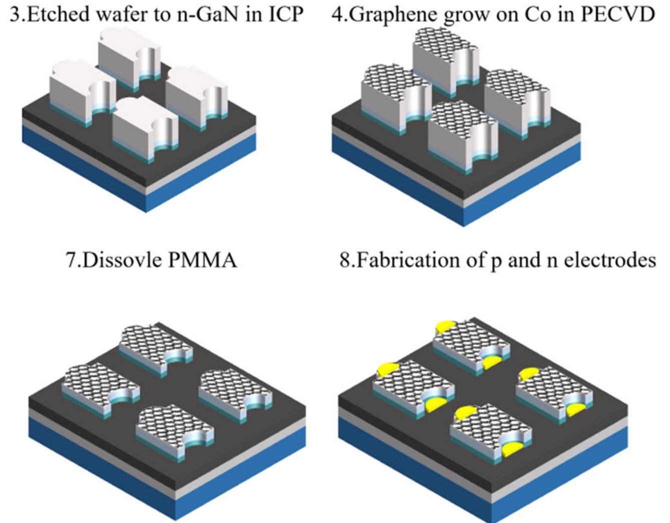

Fig. 1 The manufacturing schematic of the graphene GaN LEDs. MQW represents multi-quantum well.

investigated. The uniform as-grown graphene film is observed by scanning electron microscopy (SEM) (Fig. 2a), with the characteristic Raman peak of the sp^2 carbon atoms clearly observed (Fig. 2b). The G and 2D peaks are located at 1573 cm^{-1} and 2692 cm^{-1}, and the ratios of D/G and G/2D are measured as 0.28 and 1.99, respectively. The sheet resistance of graphene is measured in the range of 631.2–868 $\Omega\ sq^{-1}$, this resistance could potentially be improved through doping strategies in future work. The transmittance characteristics in Fig. 2c shows an average transparency of 89.84% in the range of 400–1000 wavelength. The comparison of atomic force microscopy (AFM) images among pristine GaN, GaN annealed at 600 °C, and graphene films grown on GaN at 600 °C are displayed in Fig. 2d–g, respectively. Fig. 2h is a 3D AFM image of Fig. 2f. We have found that compared with the pristine GaN roughness of 0.228 nm, GaN annealed at 600 °C has a roughness of 0.848 nm. There exists only a slight drop in the roughness (less than 1 nm). Most importantly, the roughness of graphene is measured as 0.604 nm, which demonstrates that the temperature of 600 °C does not significantly increase the roughness of either the GaN or the graphene. That is to say, the plasma enhancement reduces the temperature of graphene growth, and thus ensures the low roughness of the graphene surface. Fig. 2i, j are the Raman mapping diagrams of a 1600 μm^2 (20 × 20 points) area on the surface of graphene, where Fig. 2i represents the ratio of D/G, ranging from 0.17 to 0.75 and Fig. 2j represents the ratio of G/D, ranging from 0.87 to 3.79. Both of them confirm that the graphene has maintained a considerably high crystallization quality and flatness.

Graphene coated GaN LED analysis

From Fig. 3f–h, we have achieved nearly 100% integrity of the patterned graphene array on GaN. However, during the lift-off process of the patterned metal electrodes, when the photoresist on top of the graphene is dissolved, some graphene might be detached and damaged because the resist-graphene adhesion can be stronger at some places than others. That has brought down the final device success rate a bit, but still greater than 90%. In Fig. 3c, a mesa edge is highlighted with a solid line to guide the eye. There are no tears, wrinkles, etc. that are inevitably seen in traditional transferred graphene. Figure 3d, e shows the optical images of the graphene-GaN LEDs array after the p and n metal electrodes were deposited. Apparently, GaN LEDs with coated graphene emit light evenly over the whole p-GaN area at 20 mA injection current.

The contact resistance between graphene and p-GaN is also investigated here. Circular transfer length model (CTLM)[17–19] is used in the illustration of Fig. 4a. We have prepared six ring-shaped graphene on GaN patterns with the same inner diameter and different outer diameters by lift-off lithography and sputtering, of which the inner diameter is 76 μm and the outer diameter is 84, 90, 96, 106, 113, and 124 μm, respectively. Then *I*–*V* characteristic curves between the inside and outside graphene of the GaN ring are measured after thermal annealing at 450 °C. In the CTLM[20], the total resistance R can be given by $R = \frac{R_{sh}}{2\pi}\left[\ln\left(\frac{r_0}{r}\right) + L_t\left(\frac{1}{r_0} + \frac{1}{r}\right)\right]$, where R_{sh} is the sheet resistance of the p-GaN, r_0 and r represent the inner and outer diameters of the ring, respectively. L_t is the total length of the transmission. By using the least-squares for linear fitting the relationship between R and $\ln\left(\frac{r_0}{r}\right)$ in Fig. 4b, the slope value can be determined, which is given to R_{sh}. When $\ln\left(\frac{r_0}{r}\right) = 0$, $R_{sh} \times L_t/r\pi$ represents the intercept, and the L_t can be calculated. The contact resistivity ρ_c between the graphene and GaN can be calculated by $L_t = \sqrt{\frac{\rho_c}{R_{sh}}}$ using MATLAB programming, which is 0.421 $\Omega\ cm^2$. Although this value is still higher than that of the GaN contact to ITO, it is clearly better than those of the GaN contacts to transfer graphene[21]. Furthermore, in order to avoid any ambiguities arising from additional metals, we have not fabricated any metal electrodes on the sample. The side effect, however, is that the contacts between the graphene and the measurement probes may not be that good. This, on the other hand, indicates that the actual p-GaN to graphene contact resistivity in our experiment may be even over estimated.

To systematically study the changes that the graphene films bring to the GaN LED, pristine GaN LED without graphene is also manufactured for comparison by a similar process. As shown in Fig. 5a, the graphene-coated GaN LED reaches the current of 20 mA at 5.54 V while the pristine GaN LED needs 6.59 V in order to reach 20 mA. The gap in voltage becomes even more pronounced with the current increasing. Besides, the illustrations in Fig. 5a show optical images of the two samples operated at 20 mA, where it is clearly observed that the graphene as a highly transparent conductive electrode significantly assists the current spreading of the GaN LED surface, where the control sample only emits light nonuniformly. For further optical characterization, Fig. 5b presents the luminous flux versus the input current (Integrating sphere, EVERFINE) of the LEDs fabricated in the pristine GaN and

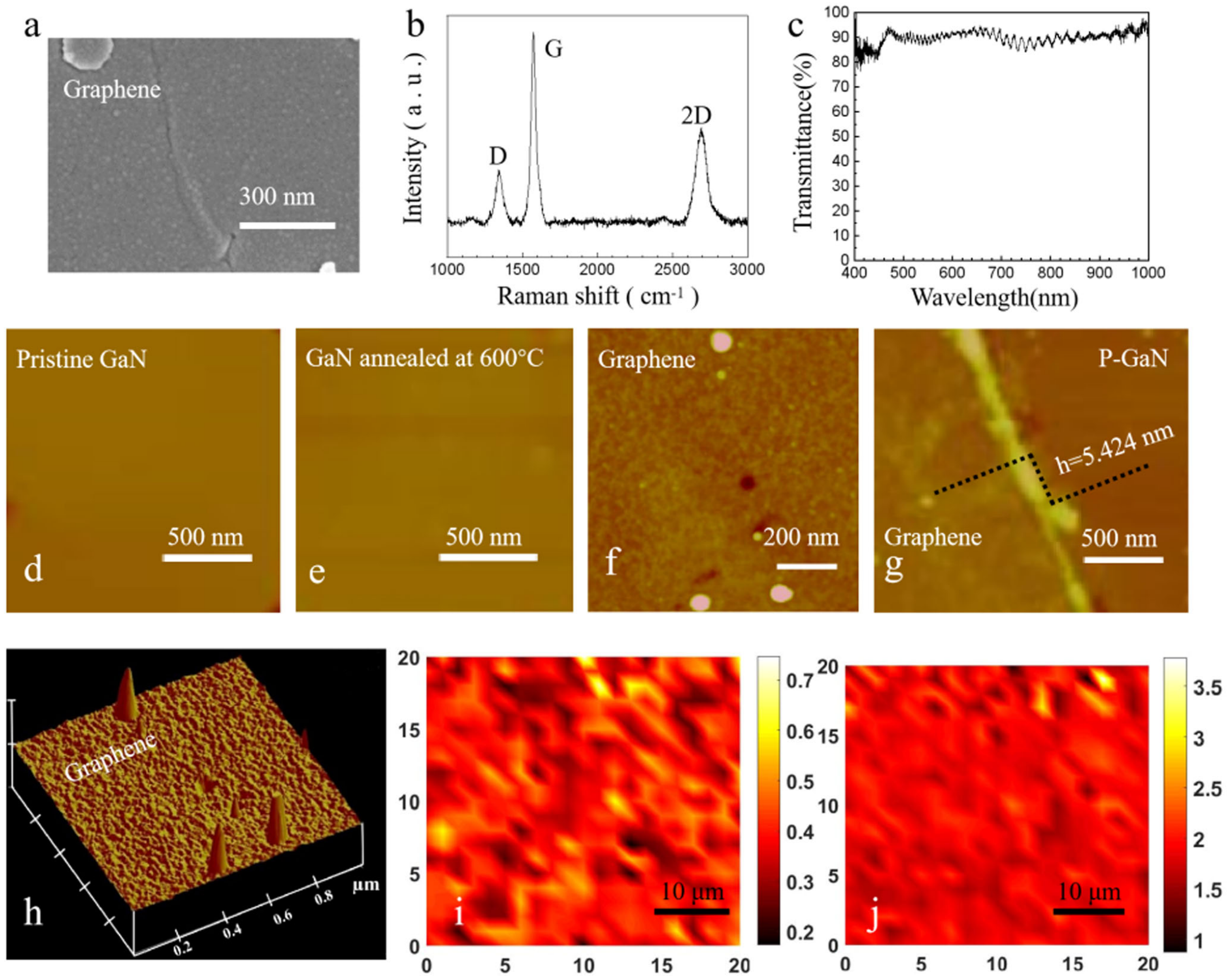

Fig. 2 Graphene thin films growth. **a** SEM image of a graphene films grown on GaN. The film is considerable uniform with few defects. **b** Raman spectra of graphene films in the range of 1000–3000 cm^{-1} where typical graphene peaks are seen. **c** Transmittance characteristics of the graphene film, showing a transmittance of ~ 90%. **d**–**g** AFM images of pristine GaN, GaN wafer annealed at 600 °C, graphene film grown on GaN, and graphene on GaN with a step. The height of graphene is nominally 5.424 nm. **h** 3D AFM image of the graphene on GaN. **i**–**j** Raman mapping of the D/G and G/2D ratios of the graphene directly grown on GaN over a 40 μm × 40 μm area (20 × 20 points), respectively.

the transfer-free graphene-coated GaN. The luminous flux of the two samples continuously increases for input current up to 100 mA. The luminous flux of the graphene-coated LED is 6 and 18% higher than the pristine GaN LED at 20 mA and 100 mA, respectively. Besides, the radiation flux of the graphene-coated LED is found to be 2.884 mW at 20 mA and 6.210 mW at 100 mA, and the radiation flux of the pristine GaN LED is found to be 2.2 mW at 20 mA and 5.053 mW at 100 mA, suggesting that the graphene-coated LED shows an improvement of 31% and 23% as compared to its counterpart at 20 mA and 100 mA, respectively. Figure 5c, d demonstrates the electroluminescence (EL) spectra of the two samples at 20 mA and 100 mA, respectively. It is clearly seen that compared with the pristine GaN LED, the full width at half maximum (FWHM) of the graphene-coated LED has been narrowed by 3.2 nm and 5.8 nm at 20 mA and 100 mA, respectively. Thus, Fig. 5b–d indicates that the graphene-coated LED generates a much stronger blue light emission with a narrower wavelength range.

The junction temperature in operation, thermal resistance[22,23] and heat spreading of the pristine GaN LED and the graphene coated GaN LED are measured at room temperature (RT) using SC7300M F/2 (MCT) and Sensing LED-201 systems to explore the thermal aspects of the devices. With a 2 mA testing current, the junction temperature and thermal resistance of the graphene coated LED are measured to be 40.25 °C and 42.25 °C W^{-1}, (the temperature coefficient K-factor is ~ 0.64 mV $°C^{-1}$), respectively, while the pristine GaN LED values are 63.61 °C and 85.8 °C W^{-1}, (K ~ 2.35 mV $°C^{-1}$), respectively. Fig. 6a, b shows the thermal map of the graphene-coated GaN LED and the pristine GaN LED operating at different current. In order to have a deeper and clearer understanding of the data, we have made line cuts (from the n electrode to the p electrode) as shown in Fig. 6a, b, and the temperature increase from RT to the working condition is plotted in Fig. 6c, d. Analyzing the results, one can see that at 20 mA the two devices have similar thermal behavior (graphene-coated LED ~ 0.61–1.36 °C, pristine GaN LED ~ 0.62–1.25 °C). However, at 100 mA, the temperature increase is much more pronounced for the pristine GaN LED as compared with its counterpart (graphene coated

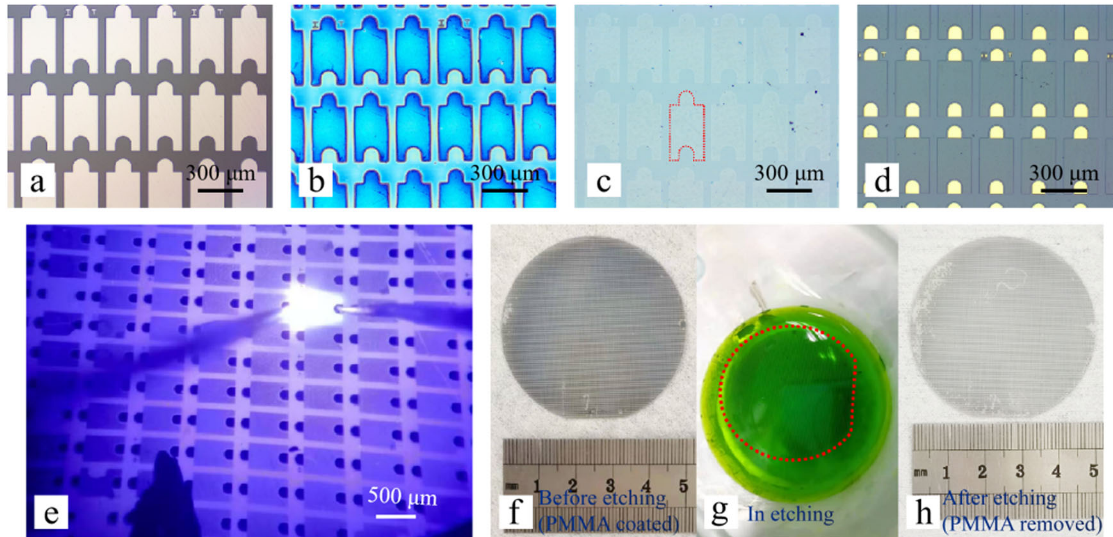

Fig. 3 Optical images taken during the actual LED preparation process. **a** Pre-prepared 300 nm Co array for the mesa etching mask and the catalyst for the graphene growth. **b** A PMMA film covers the graphene after its growth. **c** Graphene pattern array obtained by the penetration etching of Co on the p-GaN mesas. **d** P and n metal electrodes are prepared on the graphene-GaN LEDs. **e** Graphene-GaN LED glowing evenly over the whole p-GaN mesa region at 20 mA current. **f** 2-inch wafer-scale graphene array with PMMA coated. **g** Metal etching solution dissolves the Co under the PMMA and the graphene by penetration etching. **h** 2-inch wafer-scale graphene array peacefully falls on the p-GaN almost without any damage.

LED ~ 9.05–11.93 °C, pristine GaN LED ~ 11.43 °C–16.5 °C), which confirms that the graphene does help to reduce the LED junction temperature when the device is operating, thanks to graphene's excellent heat spreading ability.

As a result, the lower junction temperature and temperature increased of graphene coated LED, indicating the excellent thermal conductivity of graphene, which stems from the special delocalized pi-electrons formed by sp^2 hybridization inside graphene, resulting in lattice vibration intensifies, increased phonons, and intensified phonon scattering, thus obtaining ultra-high thermal conductivity.

In conclusion, our work demonstrated a method to grow 2-inch wafer-scale graphene pattern arrays on GaN LEDs operated as a transparent conductive layer and heat spreading layer without any transfer process. Compared with transferred graphene that is currently being practiced on GaN LEDs, our transfer-free graphene does not have the inevitable problems associated with the complicated transfer process e.g., wrinkles, tears, and holes, which is intrinsically more scalable, repeatable, and semiconductor industry compatible. The patterned Co is used both as the mesa etching hard mask as well as the graphene sacrificial catalyst in the PECVD, and therefore the graphene can be patterned without lithography. The Co can be removed peacefully by penetration etching via the PMMA and graphene. The as-grown graphene shows good electrical, optical, and heat-dissipating properties, whereas the graphene-on-GaN LEDs show better performance than the graphene-free devices. This work highlights the possible pathway of pushing graphene and other materials like SiC from the laboratory toward real industrial applications without the troublesome transfer process.

METHODS

Direct graphene synthesis on GaN LED and LED formation

The preparation schematic of the graphene GaN LEDs is shown in Fig. 1. First of all, the 2-inch wafer of the epitaxial GaN sapphire substrate was cleaned with a standard process. Second, 300 nm Co was deposited and patterned on GaN by lift-off lithography and sputtering. In the third step, Co acted as a mask for the GaN dry etching in inductively coupled plasma (ICP), and GaN was etched until heavily doped n-GaN was exposed. Then, Co acts as the catalyst for the graphene growth. We chose Co not only because Co was an excellent catalyst, but also because it almost perfectly matched the in-plane lattice constant of graphene[24]. We grew graphene at 600 °C for 3 min in plasma enhanced CVD (PECVD, Aixtron, Black Magic), which was equipped with a rapid deposition system and plasma assistance. Under a mixed atmosphere of $CH_4/H_2/Ar$ (5/20/960 sccm), 20 W (15 kHz AC) plasma was used to provide a certain portion of energy that the graphene growth needed. So, the growth temperature could be reduced to a value as low as 600 °C to avoid the indium segregation of the InGaN at high temperature. After obtaining graphene films on Co, we spun a thin layer of PMMA on the sample surface and dried it until the PMMA became solid. Then, the etching solution $CuSO_4$: HCl: H_2O = 10 g:50 mL:50 mL was used for Co etching. Here is the core technique of our work, that is, the metal etchant will penetrate the PMMA and graphene to etch the underlying Co. Although in theory graphene can be penetrated by protons only, there will inevitably be crystalline boundaries and defects in the graphene[25]. These offer the pathway for the metal etching solution via the graphene. PMMA is also known to be permeable to many types of molecules and ions[25]. Therefore, the metal etching can be accomplished smoothly. After the Co was completely etched, we removed the PMMA with acetone. Finally, p and n electrodes (Ti:20 nm, Au:500 nm) were manufactured by lift-off lithography and sputtering. The lithography of graphene is not needed at all throughout the process steps. In this way, we can realize the transfer-free graphene patterned growth in situ on the GaN LEDs, avoiding the direct contact between the photoresist and graphene, thus avoiding the severe doping on graphene. In addition, Co acted as both the mask for the etching of GaN LED mesas and the catalyst for graphene growth, significantly improving the process efficiency of the LED preparation and being

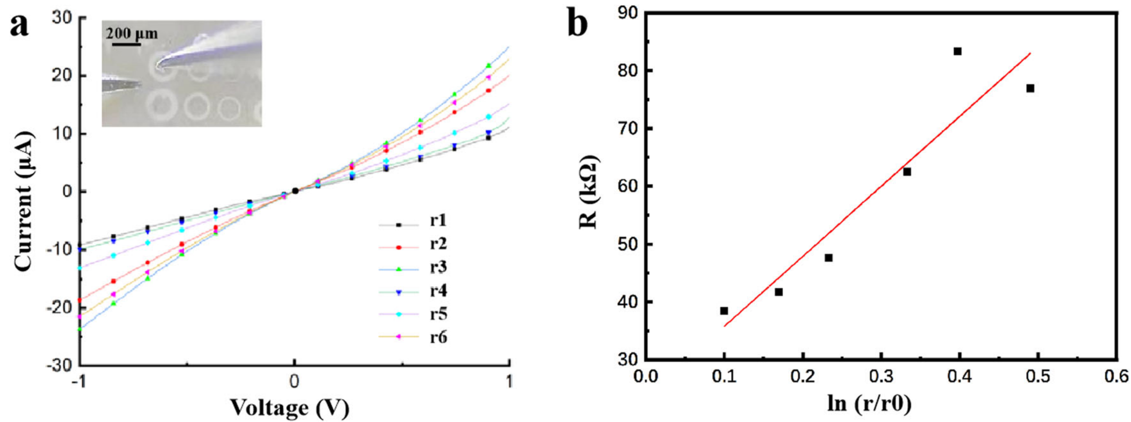

Fig. 4 The contact resistance between graphene and GaN. **a** Typical *I–V* characteristic curves for annealed graphene sheets directly grown on GaN. The illustration is optical image of the circular TLM structure. **b** The relationship between *R* on ln(*r* / *r0*).

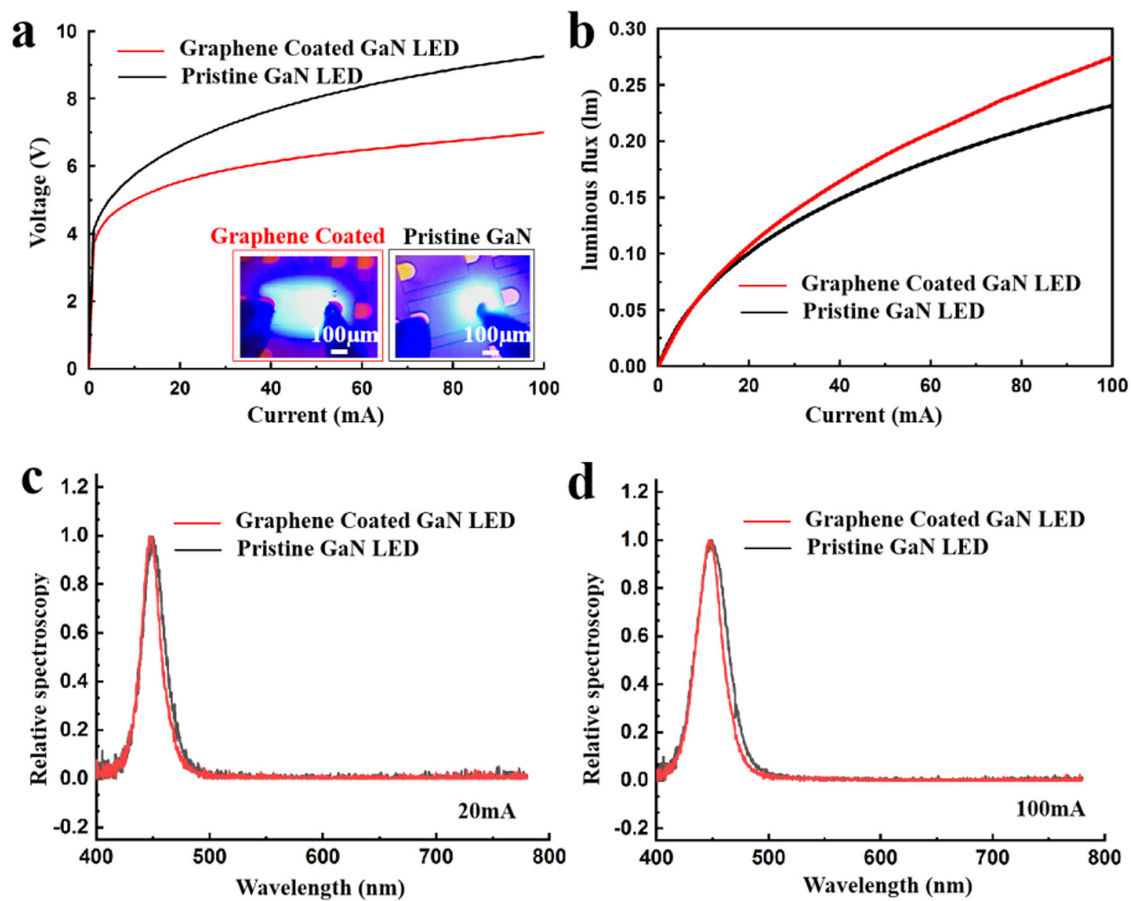

Fig. 5 Comparison of electrical and optical performance between samples. **a** *I–V* characteristics for the graphene coated LED and the pristine LED. The illustrations are optical images of the two LEDs operating at 20 mA. **b** Luminous flux of the graphene coated LED and the pristine LED at different input current. **c** EL spectra of the two LED samples at 20 mA. **d** EL spectra of the two LED samples at 100 mA.

compatible with traditional semiconductor processes. This method is simple and highly repeatable, so it is easy to achieve the growth of wafer-scale and transfer-free graphene directly on the GaN LEDs. Practically, our sample size was limited by the heater and chamber size in PEPVD and, therefore, if the equipment could be set to a larger scale, we believe that this method has the potential to achieve even larger scale GaN LEDs with transfer-free graphene.

Figure 3 shows the actual optical micrographs during the graphene LED preparation. First, as shown in Fig. 3a, we prepared a 2-inch GaN LED epitaxial wafer that is pre-deposited with a patterned 300 nm Co array for the graphene growth. Then we spin-coated the PMMA thin film on the grown graphene as shown in Fig. 3b. After the Co was removed by the penetration etching, we removed the PMMA and obtained the 2-inch wafer-scale transfer-free graphene pattern array on p-GaN in Fig. 3c, where

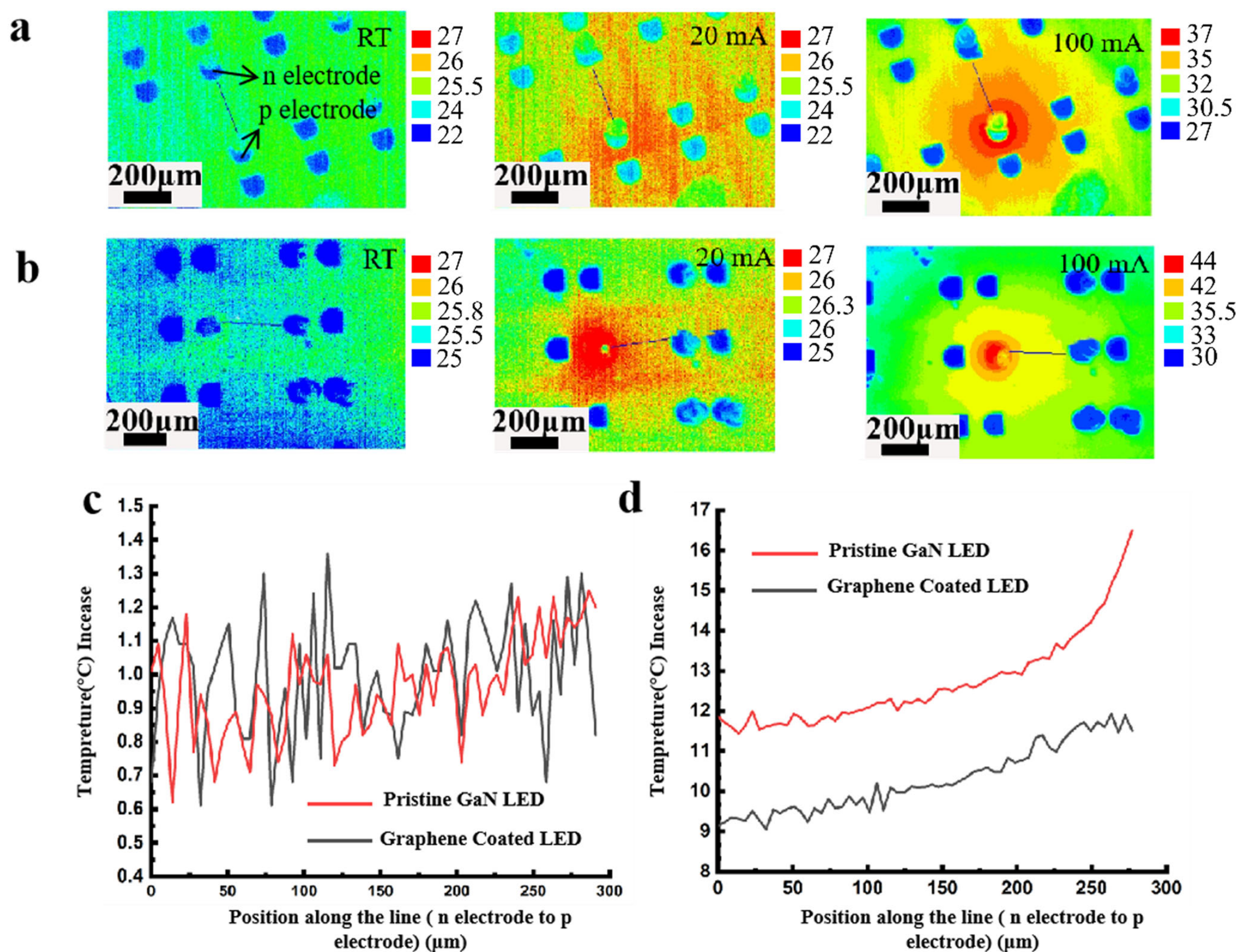

Fig. 6 Comparison of temperature distribution between samples at different current. a Temperature distribution of graphene coated LED at different current. **b** Temperature distribution of pristine GaN LED at different current. **c** The temperature increase of the two samples at 20 mA compared to room temperature. **d** The temperature increase of the two samples at 100 mA compared to room temperature.

the graphene can be seen to be almost intact before and after the Co removal, which is also demonstrated by Fig. 3f–h.

DATA AVAILABILITY

Data are available on request from the authors.

Received: 9 April 2023; Accepted: 5 October 2023;
Published online: 19 October 2023

REFERENCES

1. Novoselov, K. et al. Electric field effect in atomically thin carbon films. *Science* **306**, 666–669 (2004).
2. Bolotin, K. I. et al. Ultrahigh electron mobility in suspended graphene. *Solid State Commun.* **146**, 351–355 (2008).
3. Mak, K. F. et al. Measurement of the optical conductivity of graphene. *Phys. Rev. Lett.* **101**, 196–199 (2008).
4. Han, N. et al. Improved heat dissipation in gallium nitride light-emitting diodes with embedded graphene oxide pattern. *Nat. Commun.* **4**, 1452 (2013).
5. Bonaccorso, F., Sun, Z., Hasan, T. & Ferrarri, C. Graphene photonics and optoelectronics. *Nat. Photon.* **4**, 611–622 (2010).
6. Zhao, Y. et al. Direct growth of graphene on gallium nitride by using chemical vapor deposition without extra catalyst. *Chin. Phys. B.* **23**, 096802 (2014).
7. Sun, J., Cole, M. T., Lindvall, N., Teo, K. B. K. & Yurgens, A. Noncatalytic chemical vapor deposition of graphene on high-temperature substrates for transparent electrodes. *Appl. Phys. Lett.* **100**, 022102 (2012).
8. Sheng, Z. et al. Catalyst-free synthesis of nitrogen-doped graphene via thermal annealing graphite oxide with melamine and its excellent electrocatalysis. *ACS Nano.* **5**, 4350–4358 (2011).
9. Sun, J. et al. Direct chemical vapor deposition-derived graphene glasses targeting wide ranged applications. *Nano Lett.* **15**, 5846–5854 (2015).
10. Zhuo, Q. et al. Transfer-free synthesis of doped and patterned graphene films. *ACS Nano.* **9**, 594–601 (2015).
11. Kato, T. & Hatakeyama, R. Direct growth of doping-density-controlled hexagonal graphene on SiO_2 substrate by rapid-heating plasma CVD. *Acs Nano.* **6**, 8508–8515 (2012).
12. Sun, J. et al. A. Low partial pressure chemical vapor deposition of graphene on copper. *IEEE Trans. Nanotechnol.* **11**, 255–260 (2012).
13. Banno, K. et al. Transfer-free graphene synthesis on insulating substrates via agglomeration phenomena of catalytic nickel films. *Appl. Phys. Lett.* **103**, 666 (2013).
14. Xiong, F. et al. Transfer-free graphene-like thin films on GaN LED epiwafers grown by PECVD using an ultrathin Pt catalyst for transparent electrode. *Materials* **12**, 3533 (2019).
15. Yan, Z., Liu, G., Khan, J. M. & Balandin, A. A. Graphene quilts for thermal management of high-power GaN transistors. *Nat. Commun.* **3**, 827 (2012).
16. Zou, J., Kotchetkov, D., Balandin, A. A., Florescu, D. I. & Pollak, F. H. Thermal conductivity of GaN films: Effects of impurities and dislocations. *J. Appl. Phys.* **92**, 2534–2539 (2002).
17. Reeves, G. K. & Harrison, H. B. Obtaining the specific contact resistance from transmission line model measurements. *IEEE Electron Device Lett.* **3**, 111–113 (2005).

18. Berger, H. H. Model for contacts to planar devices. *Solid State Electron.* **15**, 145–158 (1972).
19. Reeves, G. K. Specific contact resistance using a circular transmission line model. *Solid State Electron.* **23**, 487–490 (1980).
20. Klootwijk, J. H. & Timmering, C. E. Merits and limitations of circular TLM structures for contact resistance determination for novel III-V HBTs. *Proc. IEEE 2004 Int. Conf. Microelectron. Test. Struct.* **17**, 247–252 (2004).
21. Kim, S., Lee, J. M., Lee, D. H. & Park, W. I. The effect of thermal annealing of graphene under ammonia atmosphere on its electrical properties and contact to p-GaN. *Thin Solid Films.* **546**, 246–249 (2013).
22. Pai-Ying, L. et al. Alleviation of self-heating effect in top-gated ultrathin In_2O_3 FETs using a thermal adhesion layer. *IEEE T Electron Dev.* **70**, 1 (2023).
23. Pai-Ying, L. et al. Transient thermal and electrical Co-optimization of BEOL top-gated ALD In_2O_3 FETs toward monolithic 3-D integration. *IEEE T Electron Dev.* **70**, 4 (2023).
24. Sawahata, J. et al. Structural and magnetic properties of Co doped GaN. *Phys. Stat. Sol. C* **2**, 2458–2462 (2005).
25. Dong, Y. et al. In situ growth of CVD graphene directly on dielectric surface toward application. *ACS Appl. Electron. Mater.* **2**, 238–246 (2020).

ACKNOWLEDGEMENTS

We thank the support from National Key Research and Development Program of China (No. 2023YFB3608704), Fujian Science & Technology Innovation Laboratory for Optoelectronic Information of China (No. 2021ZZ122), Hunan provincial project (No. 2020GK2064), and Fujian provincial projects (Nos. 2021HZ0114 and 2021J01583).

AUTHOR CONTRIBUTIONS

F.X. fabricated the device and conducted the measurements and data analysis. J.S. contributed to the data analysis and helped write the paper. W.G. helped revise the paper. P.T., Y.D., and Z.D. participated in the experimental design. S.F. and X.L. helped with the experimental equipment.

COMPETING INTERESTS

The authors declare no competing interests.

ADDITIONAL INFORMATION

Correspondence and requests for materials should be addressed to Jie Sun.

Reprints and permission information is available at http://www.nature.com/reprints

Publisher's note Springer Nature remains neutral with regard to jurisdictional claims in published maps and institutional affiliations.

Open Access This article is licensed under a Creative Commons Attribution 4.0 International License, which permits use, sharing, adaptation, distribution and reproduction in any medium or format, as long as you give appropriate credit to the original author(s) and the source, provide a link to the Creative Commons license, and indicate if changes were made. The images or other third party material in this article are included in the article's Creative Commons license, unless indicated otherwise in a credit line to the material. If material is not included in the article's Creative Commons license and your intended use is not permitted by statutory regulation or exceeds the permitted use, you will need to obtain permission directly from the copyright holder. To view a copy of this license, visit http://creativecommons.org/licenses/by/4.0/.

© The Author(s) 2023